RSC Advances




ROYAL SOCIETY OF CHEMISTRY

www.rsc.org/advances

# Dissociative electron attachment to the complexation ligands hexafluoroacetylacetone, trifluoroacetylacetone and acetylacetone; a comparative experimental and theoretical study.†

**Benedikt Ómarsson, Sarah Engmann and Oddur Ingólfsson***

The $\beta$-diketones acetylacetone (AAc), trifluoroacetylacetone (TFAAc), and hexafluoroacetylacetone (HFAAc), are commonly used as ligands for metal complexes in applications where relatively high stability and vapour pressure is required. While fluorination of the native AAc generally increases both stability and vapour pressure of the respective metal complexes it also alters the electronic structure, and thereby the susceptibility to bond cleavage by low energy electrons. Here we present a detailed comparative study on dissociative electron attachment (DEA) to the isolated ligands AAc, TFAAc and HFAAc in the energy range from 0-15 eV. While single bond ruptures at fairly high energies dominate in DEA to the native AAc, extensive fragmentation, new bond formation and rearrangement is observed from the fluorinated $\beta$-diketones. These reactions have high cross sections at 0 eV, where they are often associated with stabilisation through H$\cdots$F hydrogen bond formation and HF loss. From HFAAc considerable contributions are also observed at about 1 and 3 eV. Through comparison of the three compounds and quantum chemical calculations of the threshold energies for individual processes we are able to offer a plausible picture of the reaction dynamics behind the bulk of these channels. Finally, for the most dominating reaction channel, i.e., the loss of HF from HFAAc, we calculate the minimum energy path by using the nudged elastic band method.

## 1 Introduction

The $\beta$-diketone acetylacetone (AAc), and its fluorinated derivatives trifluoroacetylacetone (TFAAc) and hexafluoroacetylacetone (HFAAc) are all 2,4-pentadiones that are commonly used as complexation agents in homoleptic and heteroleptic transition metal complexes. These complexes are generally stable in air, have fairly high vapour or sublimation pressure and low decomposition temperature[1]. These properties make them suitable as precursor molecules in fabrication of nano-structures and in catalyst production by thin film preparation through chemical vapour deposition (CVD)[2,3]. More recently such $\beta$-diketone complexes have also been considered as precursor molecules for focused electron beam induced deposition (FEBID), a promising nano-fabrication method that is based on electron-induced decomposition of the precursor molecules[4,5]. In this technique the precursor molecules are decomposed close to the substrates surface using a highly focused, high-energy electron beam. However, when such an electron beam impinges on a surface the generation of low-energy secondary electrons (LESEs) is unavoidable[6]. The reactive interaction of the precursor molecules with these low energy electrons is therefore an important parameter in the deposition process. In general the energy distribution of the LESEs peaks below 10 eV[7,8], which is below the ionisation energy of most molecules. In this energy range, dissociative electron attachment (DEA) leading to incomplete decomposition of the precursor molecules can be very efficient. DEA may thus be a contributing factor in unwanted co-deposition of ligands and ligand fragments. This is of a special concern as i) the LESEs flux is high and ii) gas phase studies have shown that several precursor molecules used in FEBID have high DEA cross sections[9–12]. It is thus important to systematically characterise the reactivity of typical and potential FEBID precursor molecules with regard to their reactivity towards low-energy electrons and use this data to better understand their role in FEBID. Such detailed studies could prove useful in establishing parameters that allow targeted synthesis of precursor molecules tailored for FEBID. In this context we have recently studied DEA to the HFAAc complexes $Cu(hfac)_2$ and $Pd(hfac)_2$ [12] and compared their reactivity towards low-energy electrons with that of the native ligand HFAAc. For applications where chemical stability and fairly high vapour pressure is desirable, fluorination of AAc to give TFAAc or HFAAc may favourably alter the physical and chemical properties of their respective metal complexes. Fluorination may, however, strongly influence the electronic structure of these compounds and will generally increase their susceptibility towards reactions with low energy electrons. Furthermore, in highly fluorinated compounds, where stabilisation through intramolecular H$\cdots$F hydrogen bonds is possible, extensive fragmentation through DEA may be strongly promoted through neutral HF formation[13]. Hence, the 5.8 eV bond dissociation energy (BDE) that is released in the formation of HF makes otherwise inaccessible channels thermochemically accessible. Motivated by the potential use of $\beta$-diketone complexes in FEBID and more general by the influence of fluorination on the reac-

tivity of these compounds in their interaction with low energy electrons, we have conducted a comprehensive DEA study on HFAAc, TFAAc and AAc. We report extensive fragmentation observed in DEA to the three $\beta$-diketones and discuss these with respect to the resonances involved. For all the major fragmentation channels our discussion is supported with computed thermochemical thresholds and, in selected cases, transition state calculations along the respective reaction paths. In section 3.1, we begin by discussing in general the nature of the resonances observed in electron attachment to the three compounds. The formation of $[M-H]^-$ and the molecular anion from TFAAc is discussed in context to the effect of fluorination on the respective resonances. Subsequently, we discuss the DEA spectra of all three compounds in two separate sections. In section 3.2 we discuss dissociation channels leading to complex fragmentation through multiple bond ruptures from HFAAc and TFAAc. From AAc however, we only observe a single complex dissociation channel, i.e., all fragments except one, are formed through single bond rupture. We therefore limit the discussion of DEA to AAc to section 3.3, where we discuss the single bond ruptures observed in DEA to the three $\beta$-diketones. For each major dissociation channel we discuss the reaction path suggested to dominate the reaction dynamics.

## 2 Methods

### 2.1 Experimental

The experimental setup has been described in detail elsewhere[14] and we therefore limit our discussion here to a short description. The experimental setup is a high-vacuum apparatus where an electron beam, formed in a trochoidal electron monochromator crosses an effusive molecular beam. The liquid samples are evaporated into the vacuum chamber through an inlet system maintained at 60°C and the monochromator is held at a constant temperature of 120°C. In the experiments, we assume that the temperature of the sample gas is approximately the same as the temperature of the inlet system. The base pressure for this setup is on the order of $10^{-8}$ mbar and the working pressure was maintained at approximately $5\times10^{-7}$ mbar. The ions formed in the crossing region of the two beams are extracted by a weak ($\sim$1 V/cm) electric field towards a HIDEN EPIC 1000 mass spectrometer (Hiden analytical, Warrington UK). The electron energy scale was calibrated with respect to the formation of $SF_6^-$ from $SF_6$ at $\sim$0 eV and the incident electron energy resolution (120-140 meV) is estimated from the full width at half maximum (FWHM) of the $SF_6^-$ signal. In the current study, the appearance energy (AE) of individual fragments is estimated through linear extrapolation of the rising side of the ion yield curve, towards the baseline. The accuracy of the reported AEs is thus affected by the electron energy resolution and we therefore estimate an error of $\sim$0.2 eV. All the compounds were purchased from Sigma-Aldrich (St. Louis, MO) with a stated purity of 99% and used as delivered.

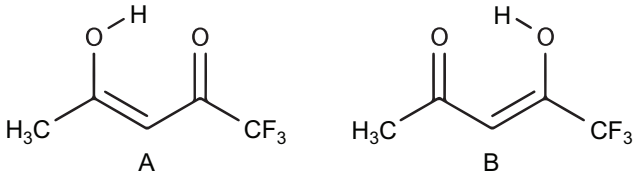


**Figure 1** The two enol conformers of TFAAc. Through thermochemical calculations we find conformer A to be 101 meV lower in energy than conformer B at room temperature, and from Boltzmann statistics, 97% of the enol conformers of TFAAc are expected to exist as conformer A at 60°C.

### 2.2 Calculations

The methods used in quantum chemical calculation of thermochemical thresholds have been described elsewhere[15] and we will therefore only give a brief description here. All geometry optimisations and single point energy calculations were performed using Orca 2.9 computational chemistry software[16]. Harmonic vibrational frequency calculations were performed with NWChem 6.1.1[17]. Thermochemical threshold values are computed on the B2PLYP[18]/ma-TZVP[19] level of theory. The zero point vibrational energy obtained from the vibrational frequency calculations is added to each species and the 0 K thermochemical threshold, $E_{th}$, is obtained by subtracting the total energy of the fragments from the total energy of the parent molecule. To account for the experimental temperature of 60 °C, the thermally corrected threshold, $E'_{th}$, is obtained by further subtracting the thermal energy of the parent molecule, at the experimental temperature, from $E_{th}$. From the vibrational frequency calculations we find this value to be 0.29, 0.35 and 0.41 eV for AAc, TFAAc and HFAAc respectively. In the gas phase at room temperature, the enol form of AAc is known to be the most stable stereoisomer[20]. Additionally, the substitution of the methyl ($CH_3$) group with $CF_3$ has been shown to shift the keto-enol equilibrium in favour of the enol isomer[21]. This is well reflected in our calculations as we find the energy difference, at room temperature, between the two isomers of the three $\beta$-diketones to be 0.27, 0.31 and 0.19 eV for HFAAc, TFAAc and AAc, respectively. Figure 1 shows two possible enol conformers of TFAAC, i.e., having the $CF_3$ group either on the keto (conformer A), or enol (conformer B) side. From our calculations we find that conformer A is 0.10 eV lower in energy than conformer B. From Boltzmann statistics this means that the enol conformers of TFAAc mainly consist of conformer A (97% at 60°C). While many differ-

ent stereoisomers exist for the $\beta$-diketones[22,23], these all constitute a negligible portion of the gas phase molecules at the current temperature. Throughout the paper, when considering thermochemical thresholds we always refer to the enol form of the $\beta$-diketones and we always refer to the thermally corrected threshold, $E'_{th}$.

To elucidate the dominating reaction channel, the minimum energy path for the formation and loss of HF was calculated using the nudged elastic band (NEB) method[24,25]. These calculations were performed using ChemShell[26] with the Orca program interfaced as QM code and the DL-FIND[27] program as a geometry optimiser. The reaction path was split into three parts, i.e., the rotation of the $-COCF_3$ group, and a two step process resulting in the formation of an anionic adduct, stabilised by hydrogen bonding between HF and the $[M - HF]^-$ moiety. Each part of the reaction path was optimised using the NEB method, with 11 images distributed along the reaction path.

## 3 Results and Discussion

### 3.1 Low energy resonances in DEA to HFAAc, TFAAc and AAc; formation of $M^-$ and $[M - H]^-$

Figure 1 shows the ion yield curves for the loss of hydrogen ($[M - H]^-$), from HFAAc, TFAAc and AAc, in the incident electron energy range from 0-15 eV. Figure 2 shows the $M^-$ ion yield from TFAAc in the same energy range. The ion yield curves for the $[M - H]^-$ and the $M^-$ formation shown in Fig. 1 and 2, respectively offer a direct comparison between the low energy contributions, observed in free electron attachment to the $\beta$-diketones. In this section we thus discuss these together, while in the following sections, the more extensive fragmentation channels will be discussed for each compound separately. A part of the DEA channels observed from HFAAc have already been described previously in a study by Engmann et al.[12], however, for completeness and clarity of the text, these will also be discussed here in context to the other $\beta$-diketones. The major contributions to the ion yield observed upon DEA to HFAAc are formed through resonances close to 0, 1 and 3 eV. At these low electron energies, core-excited resonances are rarely observed and we thus attribute the contributions close to 0 and 1 eV in HFAAc, to single electron occupation of the two lowest lying molecular orbitals. The LUMO and LUMO+1 virtual orbitals resulting from the B3LYP/ma-TZVP calculations for all three $\beta$-diketones are predominately of $\pi^*$ (A") and $\sigma^*$ (A') character, respectively. The same calculations, however, with the non-diffuse TZVP[28] basis set, gives the LUMO and LUMO+1 order of $\pi^*$ and $\sigma^*$, respectively for AAc and TFAAc but $\pi^*$ and $\pi^*$, respectively for HFAAc. Using the even more restricted 6-31G(d) basis set results in the order $\pi^*$ and $\pi^*$ for the LUMO and LUMO+1 for all three compounds. It is thus clear that the nature of the LUMO+1 resulting from our B3LYP calculations is highly dependent on the extent of the basis set used. While it's fairly clear that the LUMO in all three molecules is of $\pi^*$ character we are not confident in assigning the LUMO+1. Not withstanding the symmetry of the resonances involved, one would generally expect the resonances to be shifted towards lower energy with increasing fluorination. This is the case for the second contribution in HFAAc with respect to TFAAc while the second contribution in the ion yield of AAc does not follow this trend. We cannot offer a conclusive explanation for this behaviour, but possibly this low intensity contribution is due to a different resonance than that leading to the second contribution in TFAAc and HFAAc.

The resonance close to 3 eV we previously assigned as a core-excited resonance associated with an optically forbidden n-$\pi^*$ transition[12]. This transition was predicted by Nakanishi et al.[29] who conducted a detailed experimental study of the electronic spectrum of the three $\beta$-diketones, supported by modified CNDO calculations. The stabilisation of the negative ion resonances (NIRs), offered by increased fluorination is clearly manifested in the relative increase of the ion yield when comparing HFAAc with TFAAc and AAc. While the $[M - H]^-$ ion yield from TFAAc and HFAAc close to 0 eV is considerable, the corresponding fragment from AAc is only observed with very low yield and slightly shifted towards higher energy. The loss of hydrogen requires the rupture of a C−H or O−H bond, both being $\sigma$ bonds. In a fixed-nuclei approximation, the rupture of a $\sigma$ bond can proceed directly through a $\sigma^*$ resonance but dissociation through a $\pi^*$ resonance is symmetry forbidden. In the case of $\pi^*$ resonances, however, molecular vibrations can lead to mixing of the occupied $\pi^*$ orbital with a higher lying, unoccupied $\sigma^*$ orbital, leading to symmetry lowering of the TNI, and thus favouring the rupture of the $\sigma$ bond. This mechanism is not uncommon in DEA and has been observed in as different systems as chlorobenzene[30] and acetylene[31]. In the former, out-of-plane bending of the C−Cl bond leads to the required $\pi^*/\sigma^*$ mixing, promoting the rupture of the C−Cl bond. In acetylene, however, the same effect is achieved through bending of the molecule. This mechanism, i.e. vibronic coupling, was also suggested to play a role in the O−H rupture of formic acid, but a recent study by Janeckova et al.[32] showed that in this case, the rupture of the O−H bond proceeds directly through a short-lived $\sigma^*$ resonance (see also[33]). From the orbital assignments, we suggest that the formation of $[M - H]^-$ from the three $\beta$-diketones through the 0 eV ($\pi^*$) resonance is associated with coupling between the $\pi^*$ and the relevant $\sigma^*$ states of the TNI.

In the case of a reaction (such as the $[M - H]^-$ formation) that involves only one bond rupture, the thermochemical threshold is given by the BDE less the electron affinity (EA)

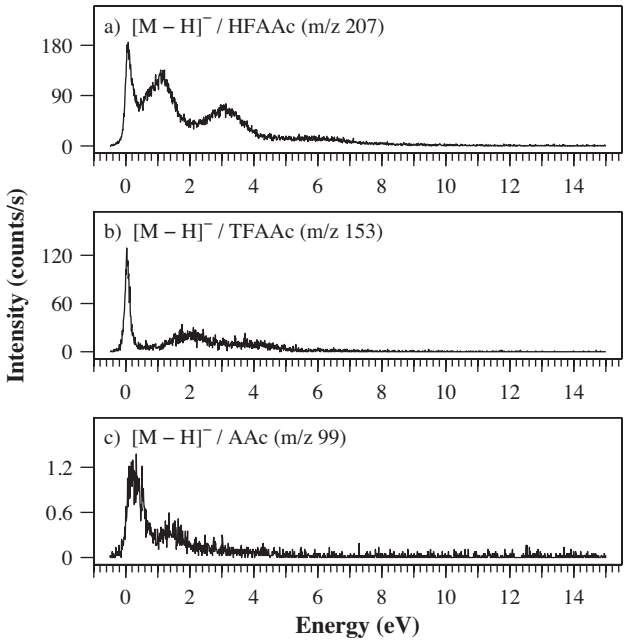


**Figure 2** Ion yield curves for the formation of $[M - H]^-$ from the three $\beta$-diketones: a) hexafluoroacetylacetone (HFAc), b) trifluoroacetylacetone (TFAc) and c) acetylacetone (AAc).

of the charge-carrying fragment, X:

$$E_{th} = \mathrm{BDE}(M-X) - \mathrm{EA}(X). \quad (1)$$

Table 1 gives the thermochemical threshold ($E_{th}$) and the thermally corrected threshold ($E'_{th}$) for the loss of hydrogen from all possible hydrogen sites of the enol form of the three $\beta$-diketones considered here (TFAc; conformer A) along with the calculated adiabatic EAs. The EAs of the three $\beta$-diketones range from −0.21 eV (AAc) to 1.62 eV (HFAAc). For the closed shell dehydrogenated anion, we expect the HOMO to be considerably more stable than the singly occupied HOMO of the molecular anion and thus we expect

**Table 1** Computed thresholds ($E_{th}$) and thermally corrected thresholds ($E'_{th}$) for the loss of hydrogen from HFAAc, TFAAc and AAc. Also listed are the calculated adiabatic electron affinities (EAs) for the three $\beta$-diketons. All values are in eV.

| Compound | EA | H-loss | $E_{th}$ | $E'_{th}$ |
|---|---|---|---|---|
| **HFAc** | 1.62 | O−H | 0.07 | −0.34 |
| | | C−H | 1.69 | 1.27 |
| **TFAc** | 0.72 | O−H | 0.82 | 0.47 |
| | | $H_2C$−H (terminal) | 1.09 | 0.74 |
| | | C−H | 2.44 | 2.09 |
| **Ac** | −0.21 | O−H | 1.25 | 0.95 |
| | | $H_2C$−H (terminal) | 1.79 | 1.49 |
| | | C−H | 3.34 | 3.05 |

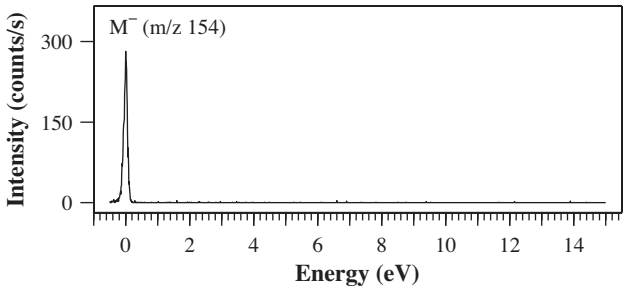


**Figure 3** Ion yield curve for the formation of $M^-$ from trifluoroacetylacetone (TFAAc).

the radical precursors to $[M - H]^-$ to exhibit high EAs. In fact, from our calculations we find the EA of [M − H] from HFAAc, where the hydrogen is lost from the oxygen, to be 4.13 eV. In DEA to HFAAc, if we assume the hydrogen loss to result from rupture of the O−H bond, we calculate a thermochemical threshold of −0.34 eV for the formation of $[M - H]^-$. The reaction is thus readily accessible at 0 eV incident electron energy. If we, however, consider the H loss from the carbon atom, we find a reaction threshold of 1.27 eV. This can be explained by the facts that the C−H bond is slightly stronger than the O−H bond[34] and that hydrogen loss from the oxygen ensures delocalisation of the electron in the conjugated $\pi$-system between the two oxygen atoms. The EA of the [M − H] radical is therefore expected to be considerably lower when the hydrogen is removed from the carbon atom. From Table 1, it is clear that in the case of HFAAc, the rupture of the O−H bond is energetically accessible through the full width of the 0 eV resonance while the rupture of the C−H bond is only energetically accessible above 1.27 eV. For TFAAc and AAc, the loss of hydrogen is possible from 3 molecular sites; the enol (O−H), the central carbon (C−H) and the terminal $CH_3$ group(s) ($H_2C$−H). For TFAAc and AAc, the formation of $[M - H]^-$ through loss of hydrogen from the oxygen is endothermic by 0.47 and 0.95 eV, respectively, while hydrogen loss from the terminal $CH_3$ group, is endothermic by 0.74 and 1.49 eV, respectively. Finally the threshold for $[M - H]^-$ formation from TFAAc and AAc through hydrogen loss from the central carbon has a threshold of 2.09 and 3.05 eV, respectively. From these thermochemical threshold values it is thus clear, that hydrogen loss from the oxygen of the $\beta$-diketones is the energetically most favourable process, however, the AEs for $[M - H]^-$ from TFAAc and AAc are at, or close to 0 eV. Considering the width of the electron beam and the accuracy of the calculations, the 0 eV contribution from TFAAc ($E'_{th} = 0.47$ eV) might result from ground state molecules. For AAc, however, the molecules contributing to the 0 eV signal must originate from the high energy tail of the Boltzmann distribution of internal energies ($E'_{th} = 0.95$ eV),

i.e., hot-band transitions. We note, that though we include the temperature of the target gas in our thermally corrected thresholds, this correction does not account for the actual internal energy distribution. Another explanation can be found in considering the presence of less stable conformers than the enol considered here. If we consider the hydrogen loss from the keto tautomer of the $\beta$-diketones we derive a thermochemical threshold of -0.61, 0.17 and 0.77 eV for HFAAc, TFAAc and AAc, respectively. As mentioned above, however, we found the energy difference between the keto and enol conformers to be 0.27, 0.31 and 0.19 eV for HFAAc, TFAAc and AAc, respectively. From Boltzmann statistics this means that only $\sim$20, 7 and 700 ppm of HFAAc, TFAAc and AAc exist in the keto-conforrmer, respectively. While this may not reflect exactly, the keto-enol ratio in the vapor phase above the liquid, it is clear that if the hydrogen loss proceeds from the keto-conformer in any of the $\beta$-diketones, the DEA cross section of this conformer is quite high.

Interestingly, the formation of the parent anion, $M^-$, through the 0 eV resonance is only observed from TFAAc (Fig. 2). In this case we attribute the extended lifetime, enabling observation of the molecular anion, to stabilisation through intramolecular vibrational energy redistribution (IVR). This is also manifested in the FWHM of the respective ion yield curves. The FWHM of the $[M-H]^-$ ion yield curve for TFAAc (Fig. 1b) is close to 180 meV and that of $[M-HF]^-$ is about 210 meV (discussed below). The FWHM of the parent anion contribution on the other hand, is close to 120 meV (Fig. 2). Hence, as is common for molecular anions formed in electron attachment, the parent anion can only be stabilised by IVR at very low energies and the FWHM observed, reflects the energy resolution of the electron beam. The fact that a metastable molecular anion is observed from TFAAc and not HFAAc or AAc can be rationalised by the stabilising effect offered through fluorination, increasing the EA. In fact, we calculate EAs of $-0.21$, 0.72 and 1.62 eV, for AAc, TFAAc and HFAAc, respectively. From the negative EA value, it is clear that AAc does not support the formation of a metastable parent anion and we thus expect autodetachment to be a dominating process. TFAAc, however, has a moderately low EA and the parent molecular anion is stabilised through IVR. For TFAAc we observe a branching ratio of IVR:DEA of about 1:10 (maximum count rates of $M^-$ vs. total ion yield at 0 eV), i.e., DEA is more favourable than IVR for TFAAc although both are operative at 0 eV. Finally, for HFAAc, the high excess energy (EA = 1.62 eV) of the parent molecular anion formed through electron attachment at 0 eV results in unfavourable conditions for IVR, and the dominating relaxation channel (besides AD) is DEA. The parent molecular anion for HFAAc is therefore not observed within the timeframe of the current experiment. This perception is supported by comparison of the EAs of these compounds with the dissociation thresholds for the low-lying channels listed in tables 1 and 2, respectively.

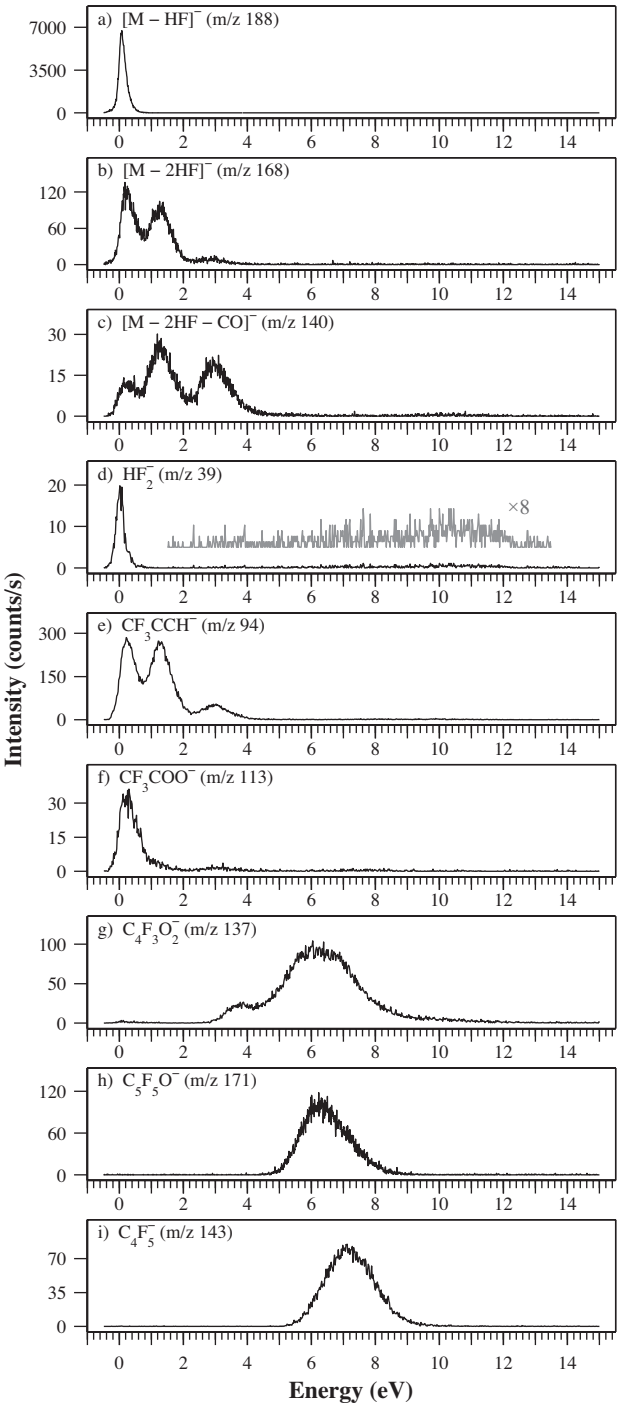


**Figure 4** Ion yield curves observed from electron attachment to HFAAc in the energy range from 0-15 eV. All the above fragments result from complex dissociation channels where bond formation and rearrangement is necessary.

**Table 2** Computed thresholds ($E_{th}$) and thermally corrected thresholds ($E'_{th}$) for all fragments observed in DEA to HFAAc, and AAc and for selected fragments observed in DEA to TFAAc. Also listed are the experimental appearance energies (AE). All values are in eV.

| Fragment | m/z | Negative | Neutral | $E_{th}$ | $E'_{th}$ | AE |
|---|---|---|---|---|---|---|
| **HFAAc** | | | | | | |
| $[M-HF]^-$ | 188 | cyclo-$C_5HF_5O^-$ | HF | -1.01 | -1.42 | 0 |
| $C_5F_5O^-$ | 171 | $F_3CC(O)CCCF_2^-$ | $HF+OH$ | 3.04 | 2.63 | 4.9 |
| $[M-2HF]^-$ | 168 | $F_3CCCC(O)C(O)F^-$ | 2HF | -0.38 | -0.79 | 0 |
| | | cyclo-$C_5F_4O^-$ | 2HF | 1.41 | 1.00 | |
| $C_4F_5^-$ | 143 | $F_3CCC(O)CF_2^-$ | $CO_2+HF+H$ | 2.58 | 2.17 | 5.5 |
| | | | $HF+OH+CO$ | 3.84 | 3.43 | 0 |
| $[M-HF-CO]^-$ | 140 | $F_3CCCC(O)F^-$ | $2HF+CO$ | 0.38 | -0.03 | |
| $C_4F_3O_2^-$ | 137 | $F_3CC(O)CCO^-$ | $CF_3+H_2$ | 1.33 | 1.04 | 2.8 |
| | | | $CHF_3+H$ | 1.30 | 1.00 | |
| $CF_3COO^-$ | 113 | $CF_3COO^-$ | $CF_3CCH_2$ | 0.23 | -0.18 | 0 |
| $C_3F_3H^-$ | 94 | $CF_3CCH^-$ | $CF_3H+CO_2$ | 0.87 | 0.46 | 0 |
| | | | $CF_3COOH$ | 1.72 | 1.31 | |
| $CF_3^-$ | 69 | $CF_3^-$ | $F_3CCOCH_2CO$ | 1.96 | 1.55 | 2.8 |
| $HF_2^-$ | 39 | $HF_2^-$ | cyclo-$C_5HF_4O$ | -0.26 | -0.57 | 0 |
| $F^-$ | 19 | $F^-$ | $F_3CC(O)CHC(OH)CF_2$ | 1.35 | 0.94 | 2.9 |
| $OH^-$ | 17 | $OH^-$ | $F_3CC(O)CHCFCF_2$ | 3.49 | 3.08 | 5.4 |
| $O^-$ | 16 | $O^-$ | $F_3CC(O)CHCHCF_3$ | 3.20 | 2.91 | 5.3 |
| **TFAAc** | | | | | | |
| $[M-HF]^-$ | 134 | cyclo-$C_5HF_5O^-$ | HF | -0.10 | -0.45 | 0 |
| $[M-2HF]^-$ | 114 | $F_3CCCC(O)C(O)F^-$ | 2HF | 0.33 | -0.02 | 0 |
| $CF_3COO^-$ | 113 | $CF_3COO^-$ | $CH_3CCH_2$ | 0.45 | 0.10 | 0 |
| $[M-CH_3CO]^-$ | 112 | $CF_3C(O)CH_2^-$ | $CH_3CO$ | 0.77 | 0.42 | 0 |
| $CF_3CCH^-$ | 94 | $CF_3CCH^-$ | $CH_4+CO_2$ | 1.08 | 0.73 | 0 |
| | | | $CH_3COOH$ | 1.65 | 1.31 | |
| $C_4H_3O_2^-$ | 83 | $C_4H_3O_2^-$ | $CF_3+H_2$ | 2.11 | 1.76 | 3.1 |
| $CH_3COO^-$ | 59 | $CH_3COO^-$ | $CF_3CCH_2$ | 1.22 | 0.88 | 0 |
| | | | $CF_2CCH+HF$ | 2.05 | 1.71 | |
| $CF_2^-$ | 50 | $CF_2^-$ | $CH_3COCH_2COCF$ | 1.95 | 1.60 | 0.8 |
| | | | $CH_3C(O)CHCO+HF$ | 2.89 | 2.54 | |
| $CH_3CCH_2^-$ | 41 | $CH_3CCH_2^-$ | $CF_3COO$ | 4.35 | 4.00 | 3.5 |
| | | | $CF_3H+H$ | 2.07 | 1.72 | |
| $HF_2^-$ | 39 | $HF_2^-$ | cyclo-$C_5HF_4O$ | -0.23 | -0.57 | 0 |
| $F^-$ | 19 | $F^-$ | $F_2CC(O)CHC(OH)CH_3$ | 1.46 | 1.12 | 3.2 |
| $OH^-$ | 17 | $OH^-$ | $F_3CC(O)CHCHCH_2$ | 2.39 | 2.04 | 6.2 |
| $O^-$ | 16 | $O^-$ | | 3.26 | 2.92 | 4.3 |
| **AAc** | | | | | | |
| $[M-CH_3CO]^-$ | 57 | $CH_3COCH_2^-$ | $CH_3CO$ | 1.67 | 1.38 | 1.2 |
| $CH_3CO^-$ | 43 | $CH_3CO^-$ | $CH_3COCH_2$ | 3.06 | 2.76 | 7.4 |
| $[M-CH_3COO]^-$ | 41 | $CH_3CCH_2^-$ | $CH_3COO$ | 3.87 | 3.58 | 7.1 |
| $OH^-$ | 17 | $OH^-$ | $H_3CCCHC(O)CH_3$ | 3.49 | 3.19 | 6.8 |
| $O^-$ | 16 | $O^-$ | $H_3CC(OH)CHCCH_3$ | 3.48 | 3.19 | 4.0 |
| $CH_3^-$ | 15 | $CH_3^-$ | $H_3CC(OH)CHC(O)$ | 3.71 | 3.42 | 7.6 |

### 3.2 Multiple bond ruptures and rearrangement reactions

As mentioned above, the stabilising effect of the fluorination on the TNIs observed in DEA to the title compounds is already apparent in the ion yield curves for the $[M-H]^-$ formation. This effect, however, becomes even more prominent when we consider the more complex fragmentation channels. While DEA to HFAAc is dominated by reactions with multiple bond ruptures and new bond formations, and most of these proceed already at 0 eV incident electron energy, single bond ruptures through higher-lying core-excited resonances play an increasing role in TFAAc. Finally, in AAc, single bond rupture through higher lying core-excited resonances govern the reaction dynamics and only one DEA channel is associated with multiple bond ruptures and new bond formations. To elucidate the dissociation dynamics of the complex DEA reactions, especially these that proceed close to 0 eV, we have calculated the reaction path for the most pronounced channel. We also calculated the relevant threshold energies for all DEA products observed from HFAAc. For TFAAc we calculated the threshold energies for reactions that we have identified as relevant for this discussion and for AAc we calculated the threshold energies for all DEA channels observed. Table 2 shows the 0 K thermochemical threshold, $E_{th}$, and the thermally corrected threshold $E'_{th}$, calculated at the B2PLYP/ma-TZVP level of theory for the channels mentioned above. Additionally, Table 2 shows the estimated experimental AE for each of the considered fragments.

#### 3.2.1 Hexafluoroacetylacetone

Figure 4 shows ion yield curves observed in DEA to HFAAc for channels where the dissociation dynamics cannot be explained by a single bond rupture. These fragments are all formed through complex dissociation reactions where multiple bond ruptures are in some cases associated with the formation of two new neutral species and rearrangement of the anionic fragment. In addition to the low energy contributions, whose nature was discussed above, significant contributions to the fragments shown in Fig. 4 are observed around 3-4, 6 and 7 eV and lesser contributions are observed close to 10 eV. We previously assigned these contributions to core-excited resonances corresponding to $\pi$-$\pi^*$, $\pi$-$\sigma^*$ and n-$\sigma^*$ excitations observed in this energy range in the near and vacuum UV spectrum of HFAAc[29]. The dominating fragment observed in DEA to HFAAc is $[M-HF]^-$ (Fig. 4a) formed with high intensity through the 0 eV resonance, e.g., the maximum count rate of $[M-HF]^-$ is about 50 times that of $[M-H]^-$. In an earlier, photolysis study of HFAAc, Basset and Whittle[35] observed a photochemical dissociation reaction leading to the loss of a hydrogen and a fluorine atom and the formation of a furanone. From thermochemical considerations, the authors argued that this reaction was concomitant to the formation of neutral HF. This argument was later supported by a tandem-chemical laser spectroscopy study by Pimentel et al.[36] who detected the neutral HF formed in the reaction. Recently, Muyskens et al.[37] showed that this reaction is also observed in photolysis of trifluoroacetylacetone (TFAAc), but the corresponding reaction leading to the formation of $H_2$ from AAc was not observed. In a sense, electron excitation from a bonding to an antibonding orbital is comparable to electron capture to the same anitbonding orbital in DEA. In recent papers we have discussed the loss of HF upon DEA from the fluorinated benzene derivatives pentafluorotoluene (PFT), pentafluoroaniline (PFA) and pentafluorophenol (PFP)[13,38]. There we showed that the existence of intramolecular $X-H\cdots F-C$ hydrogen bonds is a prerequisite for the formation of HF. In fact, for the observed HF loss in the photolysis study, Basset and Whittle[35] argued that after photon absorption, the excited HFAAc undergoes conformational changes through rotation. Hence, bringing the keto $-CF_3$ group in close vicinity to the enolic hydrogen, thus ensuring the conditions for HF formation and that of the furanone shown in Fig. 5. The same explanation holds for TFAAc, but for AAc, this reaction channel, i.e. the formation of $[M-H_2]^-$, is closed due to the lack of intramolecular hydrogen bonds along the reaction path. If we assume, that in DEA, a similar reaction path leads to $[M-HF]^-$, we calculate a threshold of $-1.42$ eV (Table 2). This reaction channel, however, is only accessible if the energy barrier, introduced through the required rotation, is surmountable. Thus, the transition state (TS) for the rotation of the $-COCF_3$ group on the anionic potential energy surface must be lower in energy than the neutral HFAAc. Fig. 5 shows the minimum energy path for the rotation of the $-COCF_3$ group from the ground electronic state of $HFAAc^-$ to that of the $-F\cdots H\cdots O-$ stabilised intermediate, the HF loss and the formation of the furanone. The rotation of the $-COCF_3$ group was optimised, using 11 images distributed along the reaction path shown in steps 1-3. Through preliminary optimisation of the rest of the path, i.e. steps 3-7, the formation of HF and closure of the 5-membered ring was found to be a two-step process, and thus the path was split in two and each part optimised through 11 images. Finally, the loss of HF shown in steps 7-8 is assumed to exhibit asymptotic behaviour. In HFAAc the transition state for the rotation is 1.16 eV above the optimised anionic enol-form at 0 K, but 0.69 eV below the corresponding neutral. After the rotation, HF loss and ring closure proceeds in a two-step process over reaction barriers that both lie below that for the rotation. The rotation is thus the rate-limiting step. For TFAAc, which EA is 0.90 eV lower than that of HFAAc, we expect the rotational transition state to lie slightly above the neutral enol conformer (about 0.2 eV). However, considering the thermal energy, it is clear that in DEA to both HFAAc and TFAAc, at 0 eV incident electron energy, HF loss followed by a spontaneous rearrangement to a 5-membered ring (furanone) is energetically favourable.

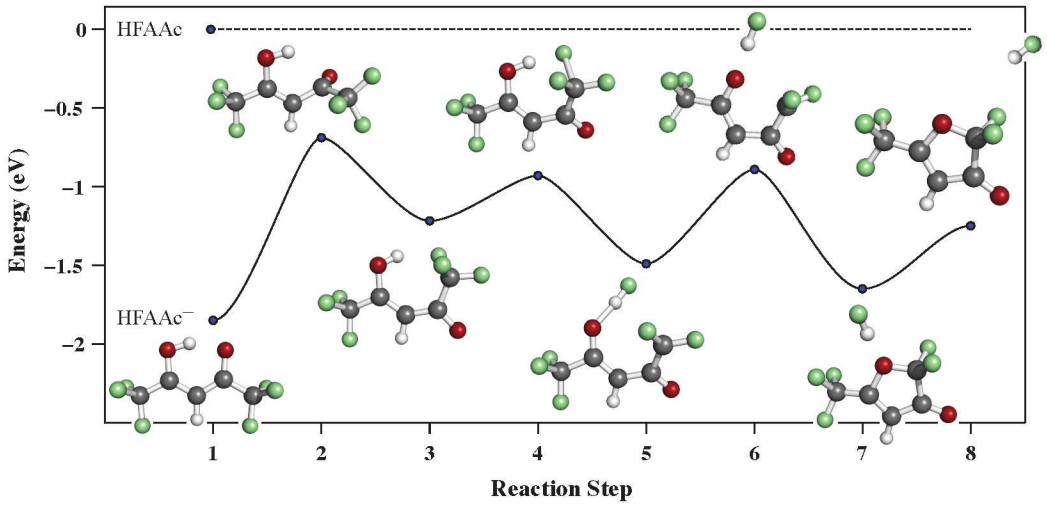


**Figure 5** The minimum energy path for the rotation of the $-COCF_3$ group of $HFAAc^-$ to form a $-F\cdots H\cdots O-$ stabilised intermediate, followed by HF loss and concomitant ring closure. The reaction path is calculated using the nudged elastic band (NEB) method. The transition state for the rotation, which is the rate limiting step, lies energetically below the neutral HFAAc, making this rotation readily available at 0 eV incident electron energy. In analogy to the mechanism proposed by Basset and Whittle[35], this rotation is proposed as a prerequisite to the loss of HF upon DEA.

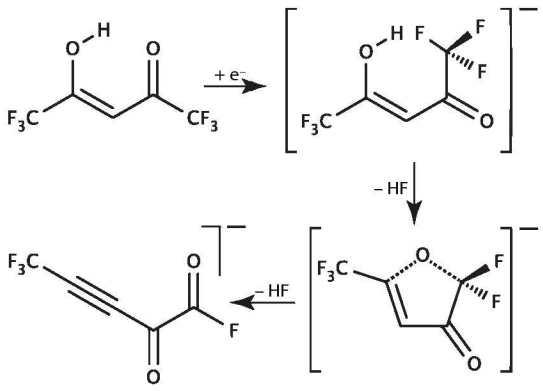


**Figure 6** Proposed reaction path and final product for the formation of $[M - 2HF]^-$ from HFAAc. Assuming the final product shown in the figure, the thermochemical threshold is found to be -0.79 eV.

Here, similar to our observations for PFP and PFA[13,38] the energy released through the formation of HF (∼5.8 eV) promotes dissociation channels, otherwise energetically inaccessible. In fact, a number of the dissociation channels observed upon electron attachment to HFAAc (see Table 2 and Fig. 4) are only energetically accessible through HF bond formation. The formation of $[M - 2HF]^-$ (Fig. 4b) formed through the 0, 1 and the 3 eV resonance, is an example of such a channel. In this case, a total of four chemical bonds are broken, a process that requires considerable energy. According to our thermochemical calculations, however, the formation of two HF may lead to a threshold that is sufficiently low for this process to proceed at 0 eV, where this fragment is observed. Originally, we expected this reaction path to involve the loss of one fluorine from each $CF_3$ group. However, the formation of $[M - 2HF]^-$ is also observed from TFAAc (see section 3.2.2), in which case both fluorines are bound to come from the same $CF_3$ group. If we assume that this reaction follows a similar path as the loss of a single HF molecule, i.e., initial rotation of the $-COCF_3$ group after electron capture, HF loss and the formation of a 5-membered ring similar to the furanone, the calculated threshold is about 1 eV. If we assume, however, that rather than closing the ring, the reaction proceeds through a path as depicted in Fig. 6, we derive a threshold of -0.79 eV. We note that the first structure of the intermediates shown in Fig. 6 represents an intermediate from the path calculated for the loss of one HF unit (step 3 in Fig 5), while the second structure is only tentative and does not necessarily represent a minimum on the actual reaction path.

With an ion yield profile, similar to that of $[M - 2HF]^-$ we also observe the fragment $[M - 2HF - CO]^-$ (Fig. 5c). This fragment is, however, formed in higher yield through the resonances close to 1 and 3 eV than through the 0 eV resonance, from which the $[M - 2HF]^-$ formation is strongest. We take this as an indication that $[M - 2HF - CO]^-$ is formed on the same or a similar reaction path as anticipated for $[M - 2HF]^-$. Hence, for this channel to proceed, an additional C–C bond must be ruptured and the fluorine must transfer to the carbonyl group next to the allyl group in the final structure in Fig. 6. Thus we expect, as observed, that the branching ratio for this channel is favoured with increas-

ing internal energy, i.e., through the higher-lying resonances. This is also supported by the threshold energy we derive for this process by assuming the formation of two HFs, CO and $CF_3-C\equiv C-CFO^-$, i.e., −0.03 eV. Such extensive fragmentation as we observe here is not unique and has been observed before in DEA to tetrafluoro-p-benzoquinone[15] where the excision of both CO groups from the quinone ring, followed by extensive rearrangement and recombination of the $C_2$ units, leads to the formation of the linear $C_4^-$ anion and two neutral $F_2CO$ molecules.

A quite interesting fragment, $HF_2^-$, is also formed in DEA to HFAAc through the 0 eV resonance (see Fig. 4d). This fragment, known as bifluoride, is a linear and symmetric anion with a 3-center, 4-electron bond between a central hydrogen and two terminal fluorines. The $HF_2^-$ anion has previously been observed in DEA to difluoroethylenes[39] and trifluoroacetone[40,41]. In HFAAc, this reaction channel requires the rupture of two C−F bonds and a single O−H bond whereas energy is gained from the F−H−F bond formation, and from the considerable EA of $HF_2$. This value has been estimated to be close to 4.8 eV[39]. In order to account for the formation of $HF_2^-$ through the 0 eV resonance we have considered a similar reaction path as for the loss of HF. In this case, however, additional fluorine is lost from the same $CF_3$ group and the reaction leads to the formation of a furanone that has one fluorine less than that formed in the case of HF loss. The thermochemical threshold obtained for this channel is −0.57 eV, supporting this reaction path at 0 eV. Further fragments observed close to 0 eV in DEA to HFAAc, are $CF_3CCH^-$ (Fig. 4e) and the trifluoroacetate anion, $CF_3COO^-$ (Fig. 4f). From a stoichiometric point of view, these fragments are complementary with regard to the retention of the hydrogen atom, and both are also formed through the resonances close to 1 and 3 eV. However, for these fragments the branching ratio is about 10/1 in favour of $CF_3CCH^-$, and while the 0 eV contribution dominates in the case of $CF_3COO^-$, the contributions through the 0 and 1 eV resonance for $CF_3CCH^-$ are of similar yield. Furthermore, the formation of $CF_3COO^-$ is not obvious from the enol conformer of HFAAc, as it requires transferring the oxygen of the hydroxyl group to the carboxyl carbon and the hydrogen of the hydroxyl group to the central carbon. Nonetheless, the thermochemically calculated threshold for this channel is −0.18 eV if we assume the complementary neutral fragment to be $CF_3CCH_2$. The formation of the trifluoroacetate, $CF_3COO^-$ is therefore thermochemically accessible at 0 eV incident electron energy given that the reaction path proceeds through transition states lower in energy than the neutral HFAAc molecule. In the case of $CF_3CCH^-$, if we assume that $CF_3COOH$ is the complementary fragment (with regard to the hydrogen retention) we calculate a threshold of 1.31 eV, and thus not accessible through the 0 eV resonance. If instead, this DEA reaction leads to the neutral fragments $CO_2$ and trifluoromethane, $CF_3H$, the thermochemical threshold is lowered to 0.46 eV. This is still higher than the observed AE, but can be rationalised by considering the energy spread of the electron beam, the fact that our thermally corrected thresholds do not account for the internal energy distribution, and by possible reaction paths with lower threshold. We thus suggest that the formation of this fragment at 0 eV is promoted through the formation of neutral $CO_2$ and trifluoromethane, $CF_3H$. We note that the formation of carbon dioxide has been observed in earlier surface-DEA experiments to small organic acids[42], we are however not aware of any such studies on $\beta$-diketones. We also note that similar to the case of $[M-H]^-$ from TFAAc and AAc, if this reaction proceeds from the keto-form of HFAAc the threshold is lowered by about 0.3 eV.

In addition to the fragments formed close to 0 eV, and through the resonances close to 1 and 3 eV, we observe $C_4F_3O_2^-$ (Fig. 4g), formed through a core-excited resonance close to 3.5 eV and through overlapping core excited resonances in the range 5-9 eV. Furthermore, $C_5F_5O^-$ (Fig. 4h) and $C_4F_5^-$ (Fig. 4i) are formed through core-excited resonances centred around 6 and 7 eV, respectively. These are most likely the same resonances that yield $C_4F_3O_2^-$ between 5 and 9 eV. Despite the comparatively high appearance energy of these fragments they cannot be formed through simple bond ruptures, but all require rearrangement and new bond formation. In turn, however, due to their comparatively high appearance energies our thermochemical threshold calculations cannot offer any conclusive insight into the nature of the fragmentation processes. We thus only list, in Table 2, the lowest thermochemical thresholds we have calculated for these and refrain from further discussion here.

#### 3.2.2 Trifluoroacetylacetone

Of the three compounds considered here, trifluoracetylacetone (TFAAc) shows the most extensive fragmentation pattern. This can in part be explained by the asymmetry of this compound compared to the other $\beta$-diketones. At the same time, TFAAc is the only compound that supports a metastable parent anion (see discussion in section 3.1). The fragmentation pattern observed for TFAAc is very similar to that observed for HFAAc and, except for the complementary $CH_3$ bearing fragments, most of the fragments observed in DEA to TFAAc are also observed in DEA to HFAAc. From TFAAc the main contributions, where rearrangement and new bond formation is required, are formed close to 0 eV incident electron energy. However, considerable contributions are also formed through core-excited resonances close to 4 and 8 eV and further overlapping core excited resonances in the range from 6-12 eV. The electronic transitions for TFAAc in the near and vacuum UV region are observed at similar photon energies as for HFAAc[29], albeit slightly shifted. Thus we expect these core-excited resonances to root in the same $\pi$-$\pi^*$, $\pi$-$\sigma^*$

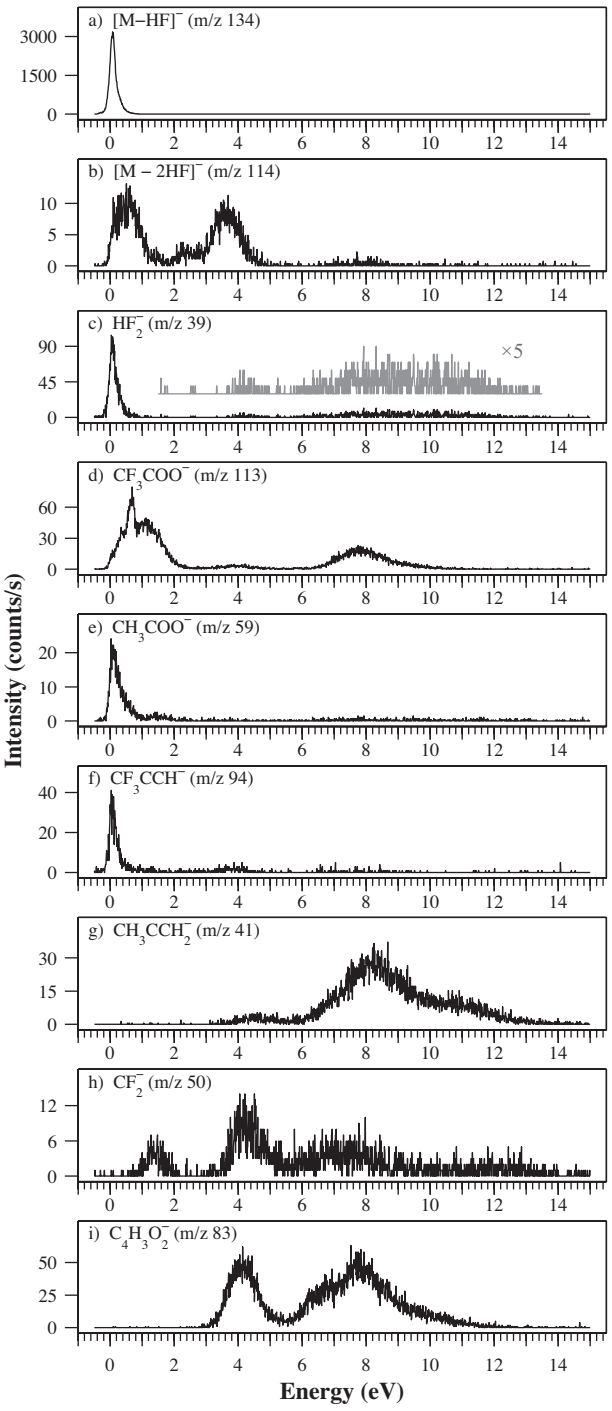


**Figure 7** Ion yield curves observed from electron attachment to TFAAc in the energy range from 0-15 eV. All the above fragments result from complex dissociation channels where bond formation and rearrangement is necessary.

and n-$\sigma^*$ excitations as is the case for HFAAc.

Figure 7 shows the ion yield curves obtained from DEA to TFAAc where the dissociation channels are governed by multiple events, involving bond ruptures, bond formations and rearrangement. Same as for HFAAc, the dominating contribution is $[M - HF]^-$ (Fig. 7a) observed close to 0 eV incident electron energy. For TFAAc we calculate a threshold of $-0.45$ eV for this reaction. The structure of the favoured TFAAc conformer (see conformer A in Fig. 3) supports rotation of the $-COCF_3$ group after electron capture, i.e. rotation is not hindered by a C=C double bond. We thus expect the reaction path to be similar to that of HFAAc, i.e., rotation to a hydrogen bonded intermediate promoting HF loss and the formation of $[M - HF]^-$ in the furanone form. In fact this reaction was also observed for neutral TFAAc in a recent photolysis study by Muyskens et al[37]. From TFAAc, we also observe $[M - 2HF]^-$ (Fig. 7b) and $HF_2^-$ (Fig. 7c) close to 0 eV resonance and we calculate the threshold for these reactions to be $-0.02$ and $-0.57$ eV respectively. Unlike HFAAc, however, the formation of these fragments from TFAAc can only result through the loss of two fluorines from the same $CF_3$ group. We thus also expect that both fluorines involved in the formation of $HF_2^-$ and $[M - 2HF]^-$ from HFAAc are from the same $CF_3$ group, as discussed above. Hence, at around 0 eV, we expect these reactions to proceed through similar paths in TFAAc and HFAAc (see Fig. 5 and 6). In addition to the 0 eV contribution, the formation of $HF_2^-$ is observed through minor contributions around 4 and from 7-12 eV. The $HF_2^-$ formation through these high-energy core-excited resonances may also be associated with the formation of a furanone, but such rearrangement is not necessary at these energies. In addition to the fragments discussed here above, trifluoroacetate ($CF_3COO^-$), acetate ($CH_3COO^-$) and $CF_3CCH^-$, are also observed from TFAAc, at or close to 0 eV (see Fig. 7d-f). From these, $CF_3COO^-$ is the only fragment with appreciable yield, formed through the higher lying core-excited resonances, i.e., at about 4 and 8 eV. The reaction path, leading to the formation of $CF_3COO^-$ is expected to be similar to that for HFAAc and the thermochemical threshold is found to be 0.10 eV if we assume the neutral fragment $CH_3CCH_2$. The anionic counterpart, $CH_3CCH_2^-$ (Fig. 7g) (complementary to $CF_3COO^-$) is only formed through the higher lying core excited resonances, i.e., with low yield from slightly below 4 to about 6 eV and through overlapping resonances from about 6-12 eV. Assuming the same reaction path as for the formation of $CF_3COO^-$, with the charge retention at the $CH_3CCH_2$ moiety, we find the thermochemical threshold to be 4.0 eV, which is in fairly good agreement with the ion yield curves observed. If the formation of $CH_3COO^-$ from the most stable conformer of TFAAc proceeds in a similar way to the $CF_3COO^-$ formation, now with a neutral $CF_3CCH_2$ fragment, we derive a threshold of 0.88 eV. We also considered the formation of

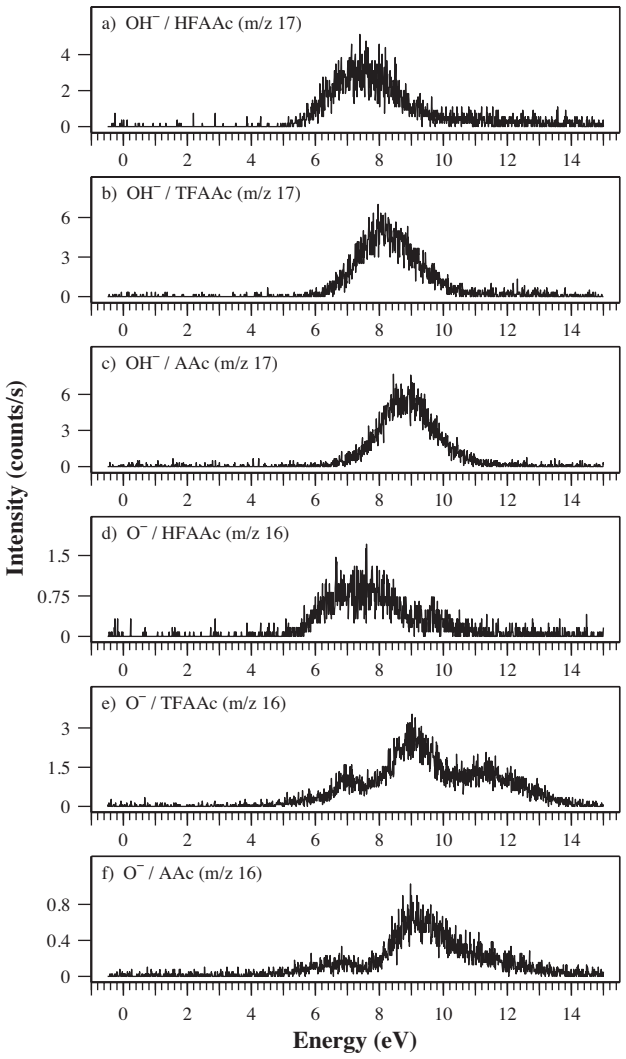


**Figure 8** Ion yield curves for the formation of $OH^-$ and $O^-$ from HFAAc, TFAAc and AAc in the energy range from 0-15 eV.

HF and a $CF_2CCH$ radical, but this channel we find to be endothermic by 1.71 eV. Finally, for $CF_3CCH^-$, similar to its formation from HFAAc, we derive a threshold of 1.31 eV if we assume the neutral fragment to be $CH_3COOH$. However, considering the formation of $CO_2$ and methane $CH_4$ results in a threshold of 0.73 eV. The threshold values we calculate for $CF_3CCH^-$ and for $CF_3COO^-$ are markedly higher than the observed AE. This might be explained by considering the keto tautomer or hot-band transitions, as mentioned above.

Finally the fragments $CF_2^-$ (Fig. 7h) and $C_4H_3O_2^-$ (Fig. 7i) are observed from TFAAc. Both are formed through the core-excited resonances close to 4 eV and between 6 and 10 eV, and $CF_2^-$ is also formed between 1 and 2 eV. The formation of $CF_2^-$ requires the rupture of the $C-CF_3$ bond

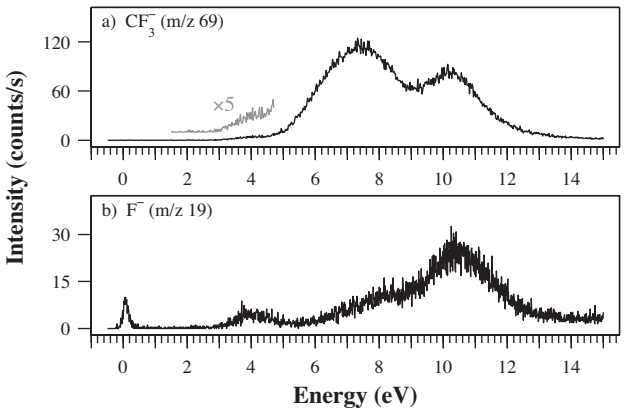


**Figure 9** Ion yield curves for a) $CF_3^-$ and b) $F^-$ observed from electron attachment to HFAAc in the energy range from 0-15 eV. Apart from $[M-H]^-$ (figure 1), $OH^-$ and $O^-$ (figure 8), these are the only fragments formed through single bond rupture in DEA to HFAc.

and the additional loss of a fluorine. The lowest threshold we find for this fragment is 1.60 eV and includes formation of acetoacetyl fluoride ($CH_3COCH_2C(O)F$). Assuming the formation of $CF_2^-$ involves the formation of HF and acetylketene ($CH_3C(O)CHCO$) we, however, find the threshold to be 2.45 eV. The fragment $C_4H_3O_2^-$, on the other hand, has a fairly high AE and can be associated with the formation of trifluoromethane ($CF_3H$), but also the formation of $CF_3$ and $H_2$ results in a threshold well below the observed AE (see Table 2).

### 3.3 Single Bond Ruptures

From the fragments formed through the rupture of a single bond upon DEA to HFAAc, TFAAc and AAc, only the fragments $OH^-$ and $O^-$ are observed from all three. For this reason and the fact that the $OH^-$ yield reflects the degree of fluorination of the three $\beta$-diketones very clearly, we will discuss these before discussing the remaining fragment for each $\beta$-diketone separately. Figure 8 shows the $OH^-$ ion yield curves from HFAAc, TFAAc and AAc in panel a), b) and c), respectively, and that of $O^-$ in panels d), e) and f), respectively. The formation of $OH^-$ is observed through a single contribution which shape and width is similar for all compounds. The onset and the maximum, on the other hand, is successively shifted to higher energy when proceeding from HFAAc through TFAAc to AAc. In the ion yield curve for HFAAc the maximum is close to 7.4 eV, in that for TFAAc close to 8.1 eV and from AAc close to 8.8 eV. Similar trend is observed for the onset of this contribution. In a previous photochemical study, Yoon et al. observed the spontaneous loss of OH from HFAAc (and Ac), upon electronic excitation by photon irradiation in the

range from 312-290 nm (3.98-4.28 eV)[43]. The authors attributed the excitation to a $\pi$-$\pi^*$ transition observed as a broad structure, centred at 4.72 eV in the UV spectrum[29]. In a later photodissociation study on AAc, Upadhyaya et al.[44] observed the loss of OH at 193 nm (6.43 eV), which they attributed to a dissociation resulting from an excitation to a $\sigma^*$ repulsive state. In accordance with the photochemical study by Upadhyaya et al.[44] we attribute the formation of $OH^-$ in DEA to HFAAc, to a core-excited $\sigma^*$-type resonance from the enolic part of HFAAc. This contribution is successively shifted to lower energy as the degree of fluorination increases. We note, however, that we calculate the thermochemical threshold for the formation of $OH^-$ from all three $\beta$-diketons, to be slightly above 3 eV. Thus, in principle this channel should be accessible in the energy range where Yoon et al.[43] observe OH loss in their photodissociation study, i.e., around 4 eV. We cannot offer any definitive reason for the lack of $OH^-$ formation in this energy range, especially for HFAAc and TFAAc where other fragments are observed in this energy range. However, a possible explanation can be in the high activation barrier we expect for $OH^-$ loss from the enolic form due to the hydrogen bond.

The formation of $O^-$, from all three compounds, is observed through multiple contributions, centred around 7, 9 and 11.5 eV. The 7 eV contribution is by far the dominating one from HFAAc while the 9 eV contribution dominates from both TFAAc and AAc. Finally the 11.5 eV contributions is only significant in the $O^-$ ion yield from TFAAc. In our calculations, optimisation of the neutral [M − O] results in hydrogen transfer from the enolic oxygen to the carbon atom that contained the keto oxygen and the thermochemical threshold for this channel is found to be about 3 eV for all three $\beta$-diketones. We attribute the formation of $O^-$ from HFAAc to result from multiple core-excited $\pi^*$ and $\sigma^*$ type resonances.

#### 3.3.1 Hexafluoroacetylacetone

Figure 9 shows the ion yield curves for $CF_3^-$ and $F^-$ from DEA to HFAAc. Beside $[M - H]^-$, $OH^-$ and $O^-$, these are the only fragments observed from HFAAc, which formation may be explained by single bond ruptures. While the dominating, $[M - H]^-$, is mainly formed through the 0 eV resonance, as discussed in section 3.1, all other fragments that result from a single bond rupture are exclusively formed through the high-energy core-excited resonances. This applies to $OH^-$ and $O^-$, as discussed above, and to $F^-$ and $CF_3^-$, which are both formed through a core-excited resonance close to 4 eV and a number of core excited resonances between 5 and 13 eV. The experimental AE for the formation of $CF_3^-$ and $F^-$ is in both cases close to 3 eV, and their calculated thermochemical thresholds are 1.55 and 0.94 eV, respectively. Hence, both these channels are readily accessible at their respective AEs. In addition to the high-energy contributions, a small signal in the ion yield curve of $F^-$ is observed close to 0 eV. We attribute this to $F^-$ from $CF_3$ radicals formed at the hot filament, as has been discussed earlier[12], and not to a contribution from HFAAc.

#### 3.3.2 Trifluoroacetylacetone

Figure 10 shows ion yield curves for fragments formed through single bond rupture in DEA to TFAAc. The fragmentation observed is more extensive than that from HFAAc, and in addition to the fragments $OH^-$ and $O^-$ discussed above, and the fragments $CF_3^-$ (Fig. 10a) and $F^-$ (Fig. 10b) which are also formed from HFAAc, we observe a series of four fragments. These are $CH_3CO^-$ (Fig. 10c), $[M - CH_3CO]^-$ (Fig. 10d), $CF_3O^-$ (Fig. 10e) and $[M - CF_3CO]^-$ (Fig. 10f), and can be associated with C=C and C−C bond ruptures at the enol and keto side of TFAAc, respectively. In TFAAc, the main contributions to the ion yields of $CF_3^-$ and $F^-$ are formed through resonances close to 8 eV and a lesser contribution is formed close to 4 eV. In the vacuum UV spectrum of TFAAc, an n-$\sigma^*$ transition is observed at 9.7 eV[29] but in DEA to TFAAc, we do not observe the formation of $CF_3^-$ from a core-excited resonance in this energy range, and $F^-$ is only formed with low intensity close to 10.5 eV. This is in contrast to HFAAc (see Fig. 9) where a prominent contribution to the ion yields of $F^-$ and $CF_3^-$ is observed close to 10.5 eV. We attribute this to a lesser stabilisation of the 10.5 eV resonance in TFAAc, due to lower degree of fluorination, thus allowing autodetachment to compete more effectively with dissociation in this energy range. We find the thermochemical threshold for this channel to be 0.42 eV. If we consider this reaction to take place from the keto tautomer, however, the threshold is lowered to 0.12 eV and we would also expect the activation barriers to be lower. The complementary fragment, $CH_3CO^-$, is also formed, but only with low intensity and through the core-excited resonances close to 4, 8 and 11 eV. We have not calculated the threshold for this fragment explicitly for TFAAc but for AAc we find a threshold of 2.76 eV and we expect the threshold to be similar for TFAAc. Finally, the fragment $CF_3CO^-$ is formed through the core-excited resonance around 8 eV and the complementary fragment, $[M - CF_3CO]^-$, is observed around 4, 8 and 11 eV. The ion yield of both these fragments is, however, very low.

#### 3.3.3 Acetylacetone

Figure 11 shows the ion yield curves observed in DEA to acetylacetone (AAc) in the energy range from 0-15 eV incident electron energy. Table 2 lists the corresponding threshold energies calculated at the B2PLYP/ma-TZVP level of theory. All fragments are observed with low intensity compared to HFAAc and TFAAc, the highest ion yield being that of $OH^-$ shown in Fig. 8c and discussed here above (section 3.3). Apart from $[M - CH_3COO]^-$ (Fig. 11d), all the observed fragments are considered to result from single bond rupture after electron attachment and, only $[M - H]^-$ (section

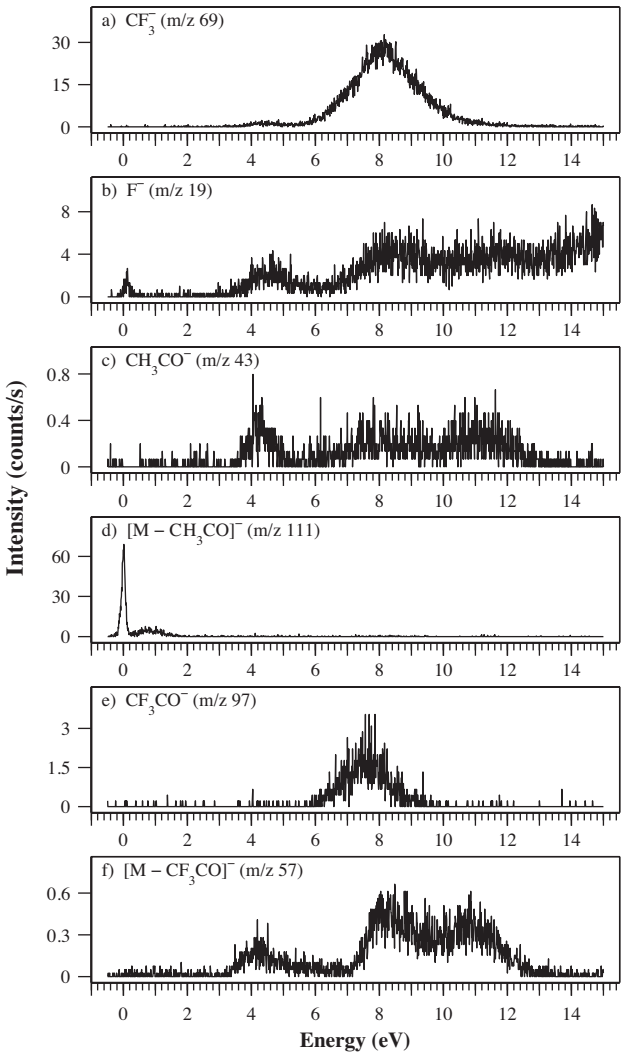


**Figure 10** Ion yield curves corresponding to fragments formed through single bond rupture in DEA to TFAAc. In addition to the above $[M - H]^-$ (figure 1), $OH^-$ and $O^-$ (figure 8) are also observed.

3.1), is observed close to 0 eV. All other fragments are exclusively formed through the high-lying core-excited resonances. The limited dissociation channels available through the low-energy resonances in DEA to AAc is readily explained from thermochemical considerations as can be seen from Table 2. For DEA reactions involving a single bond rupture to occur at 0 eV, equation (1) shows that the EA of the charge-carrying moiety must compensate for the energy required to rupture the respective chemical bond. This is in fact quite rare and usually limited to cases involving leaving groups with high EAs (Cl, Br, I and CN; see for example the review articles[45,46]). Apparently, with the exception of [M − H], no other observed fragment has sufficient EA to be formed through single bond rupture close to 0 eV. In addition to $[M - H]^-$, the fragment $[M - CH_3CO]^-$ (Fig. 11a) shows minor contributions through the low-energy shape resonance, i.e. from 1.3-2.5 eV. The fragment is also observed through a minor contribution from 4-6 eV and finally a fair contribution from 7-11 eV. In the geometry optimisations of $[M - CH_3CO]^-$, we find that rather than stabilising as an enol radical, a transfer of the enolic hydrogen to the carbon atom, forming the $CH_3COCH_2^-$ anion is preferred. Considering this hydrogen transfer we derive a threshold of 1.38 eV, which agrees well with our observations. The complementary reaction, the formation of $CH_3CO^-$ (Fig. 11b) is only a minor dissociation channel, observed from 7.5-10 eV. This can be explained by the low EA of the $CH_3CO$ radical (0.42 eV)[47], which does not compensate for the C−C bond rupture. Accordingly, the computed thermochemical threshold for this dissociation channel is 2.76 eV and the reaction is thus thermochemically inaccessible through the low-lying resonances. Terminal bond rupture leading to the formation of $CH_3^-$ (Fig. 11c), is also observed from AAc, and this fragment appears through a single contribution peaking close to 9 eV. The thermochemical threshold, for this channel is 3.42 eV, hence, well below the AE of the fragment.

Finally, the fragment $[M - CH_3COO]^-$ is formed through the core-excited resonance close to 9 eV. This is the only fragment we observe from AAc that requires multiple bond ruptures and new bond formation. Considering the anion $CH_3CCH_2^-$ and the neutral counterpart $CH_3COO$ we derive a threshold of 3.58 eV, which is well below the observed AE. The loss of $CH_3COO$ was not observed in DEA to TFAAc, although we did observe $[M - CF_3COO]^-$, hence the formation of the anion $CH_3CCH_2^-$. Interestingly, from HFAAc where this fragment ($CH_3CCH_2^-$) cannot be formed, the corresponding loss of $CF_3COO$ is not observed.

In addition, to the fragments discussed above, we have also looked for $H^-$ formation from AAc. While we cannot efficiently extract $H^-$ in our current experimental setup due to the high magnetic field, we were still able to detect $H^-$ from AAc through the high-energy resonances. Due to large background signal, however, and a large error in the electron energy due to the strong extraction field needed to extract the $H^-$ ion, we feel the data is ill suited for publication at this stage and we refrain from further discussion on the energy dependence of the $H^-$ formation.

## 4 Conclusions

In low energy electron interaction with the $\beta$-diketones; acetylacetone, trifluoroacetylacetone and hexafluoroacetylacetone electron attachment leads predominantly to fragmentation and within the time window of the current experiments, the molecular anion is only observed from TFAAc. The degree of fluorination is clearly reflected in the dissociation reactions of

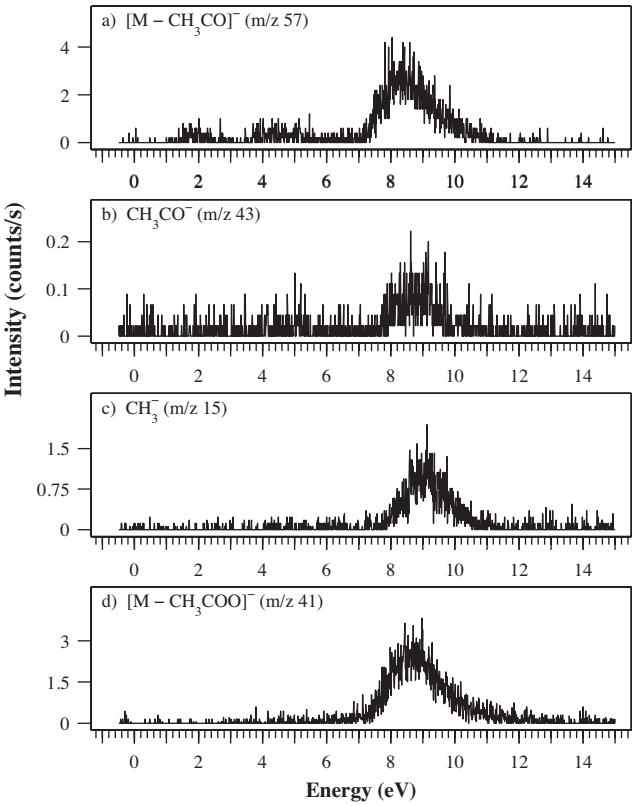


**Figure 11** Ion yield curves from DEA to acetylacetone (AAc) in the energy range from 0-15 eV. Apart from panel d) which represents a complex dissociation channel, all the fragments can be formed through single bond rupture. In addition to the above fragments, [M − H]$^-$ (figure 1), OH$^-$ and O$^-$ (figure 8) are also observed.

the respective compounds, i) through stabilisation of the NIRs involved and ii) through facilitation of fragmentation by HF formation. The second effect, in conjunction with quantum chemical calculations, allows us to explain the reaction paths behind the formation of a number of the fragments observed. While DEA to AAc is characterised by single bond ruptures that proceed with low cross sections through core-excited resonances at fairly high energy (>4 eV), DEA to TFAAc leads to about the same number of fragments through single bond ruptures as through complex rearrangement reaction. The rearrangement reactions, however, proceed mainly at low energies and generally with considerably higher cross sections. Finally, DEA to HFAAc is dominated by complex rearrangement reactions through the low energy resonances, both with respect to the number of fragments and the cross section for the individual processes. The main channel in DEA to both TFAAc and HFAAc is the formation of HF but also the loss of two HFs and the formation of $HF_2^-$ are observed, though with considerably less intensity. Our threshold and nudged elastic band (NEB) calculations show that the channels leading to the loss of HF are enabled through an O···H···F intermediate leading to the formation of a furanone-like compound concomitant to the HF loss. While $HF_2^-$ formation most likely proceeds through a similar path, the loss of two HFs, leads to an open chain anion. It is worth noting that the $HF_2^-$ formation and the loss of two HFs proceed to similar extent from TFAAc and HFAAc, and both fluorines lost through the respective channels are thus likely to be from the same $CF_3$ group. The main contribution to the ion yield from HFAAc and TFAAc is observed close to 0 eV, while considerable contributions from HFAAc are also observed close to 1 and 3 eV.

It is clearly demonstrated here that the degree of fluorination increases the DEA cross section considerably, a phenomena that is fairly well understood and is common to most organic compounds. However, in conjunction to our previous studies, it is also clear that by introducing the stereochemical prerequisites for an energetically accessible hydrogen bonded X···H···F intermediate on the DEA reaction path, molecular fragmentation may be significantly enhanced through HF formation. We thus propose that introducing such predetermined breaking points into molecular systems, may be used to increase the molecules' sensitivity to bond breakage by low energy electrons and even control their reactivity towards these. As pointed out in the introduction, DEA can be disadvantageous in FEBID as secondary (back-scattered) electrons can contribute to deposit-impurities through incomplete dissociation of the precursor molecules. However, we point out that the main fragmentation channels we observe in the current study are promoted through the formation of HF. In a recent study by Engmann *et al.* [12], these reaction channels were shown to be closed when the deprotonated HFAAc is bound as a bidendate ligand in the metal-complexes Cu(hfac)$_2$ and Pd(hfac)$_2$.

Enhancing the DEA fragmentation efficiency of radiosensitisers used in cancer therapy may also prove beneficial. Halogenated radio sensitisers such as 5-halouracils[48] have been proposed to owe their effectiveness to increased electron attachment cross section leading to low energy electron induced damaged to the DNA. Increasing the DEA cross section of radiosensitisers through the introduction of predetermined breaking points, could thus increase the effectiveness of radiosensitisers in ion beam cancer therapy.

## 5 Acknowledgements

The authors acknowledge financial support from the Icelandic Centre for Research (RANNÍS) and the University of Iceland Research Fund. We would like to thank Birkir Reynisson for his contribution to the measurements and Frímann Haukur Ómarsson for estimating the appearance energies. This work was conducted within the framework of the COST actions

MP1002 on Nanoscale Insights into Ion Beam Cancer Therapy and CM1301 on Chemistry for Electron-Induced Nanofabrication.

## References


1 R. E. Sievers and J. E. Sadlowski, *Science*, 1978, **201**, 217–223.
2 J.-Y. Zhang and H. Esrom, *Appl. Surf. Sci.*, 1992, **54**, 465–470.
3 T. Maruyama and T. Shirai, *Journal of materials science*, 1995, **30**, 5551–5553.
4 I. Utke, P. Hoffmann and J. Melngailis, *J. Vac. Sci. Technol. B*, 2008, **26**, 1197–1276.
5 W. F. Van Dorp and C. W. Hagen, *Journal of Applied Physics*, 2008, **104**, 081301–081301–42.
6 N. Silvis-Cividjian, C. W. Hagen and P. Kruit, *Journal of Applied Physics*, 2005, **98**, 084905.
7 T. Koshikawa and R. Shimizu, *Journal of Physics D: Applied Physics*, 1973, **6**, 1369.
8 J. Schaefer and J. Hoelzl, *Thin Solid Films*, 1972, **13**, 81–86.
9 S. Engmann, M. Stano, S. Matejčík and O. Ingólfsson, *Angew. Chem. Int. Ed.*, 2011, **50**, 9475–9477.
10 O. May, D. Kubala and M. Allan, *Phys. Chem. Chem. Phys.*, 2012, **14**, 2979.
11 S. Engmann, M. Stano, S. Matejčík and O. Ingólfsson, *Phys. Chem. Chem. Phys.*, 2012, **14**, 14611–14618.
12 S. Engmann, B. Ómarsson, M. Lacko, M. Stano, S. Matejčík and O. Ingólfsson, *J. Chem. Phys.*, 2013, **138**, 234309.
13 B. Ómarsson, E. H. Bjarnason, O. Ingólfsson, S. Haughey and T. A. Field, *Chem. Phys. Lett.*, 2012, **539-540**, 7–10.
14 E. H. Bjarnason, B. Ómarsson, S. Engmann, F. H. Ómarsson and O. Ingólfsson, *Eur. Phys. J. D*, 2014, **68**, 121.
15 B. Ómarsson and O. Ingólfsson, *Phys. Chem. Chem. Phys.*, 2013, **15**, 16758–16767.
16 F. Neese, *WIREs Comput Mol Sci*, 2011, **2**, 73–78.
17 M. Valiev, E. J. Bylaska, N. Govind, K. Kowalski, T. P. Straatsma, H. J. J. Van Dam, D. Wang, J. Nieplocha, E. Apra, T. L. Windus and W. A. de Jong, *Comput. Phys. Commun.*, 2010, **181**, 1477–1489.
18 L. Goerigk and S. Grimme, *J. Chem. Theory Comput.*, 2011, **7**, 291–309.
19 J. Zheng, X. Xu and D. G. Truhlar, *Theor. Chem. Acc.*, 2010, **128**, 295–305.
20 H. Nakanishi, *Bull. Chem. Soc. Jpn.*, 1977, **50**, 2255–2261.
21 J. L. Burdett and M. T. Rogers, *J. Am. Chem. Soc.*, 1964, **86**, 2105–2109.
22 N. Nagashima, S. Kudoh and M. Nakata, *Chem. Phys. Lett.*, 2003, **374**, 59–66.
23 S. Coussan, Y. Ferro, A. Trivella, M. Rajzmann, P. Roubin, R. Wieczorek, C. Manca, P. Piecuch, K. Kowalski, M. Włoch, S. A. Kucharski and M. Musiał, *J. Phys. Chem. A*, 2006, **110**, 3920–3926.
24 H. Jónsson, G. Mills and K. W. Jacobsen, *Classical and Quantum Dynamics in Condensed Phase Simulations*, World Scientific, Singapore, 1998, p. 385.
25 H. Jónsson, *Proc. Natl. Acad. Sci.*, 2011, **108**, 944–949.
26 *Chemshell, a Computational Chemistry Shell, see: www.chemshell.org*.
27 J. Kästner, J. M. Carr, T. W. Keal, W. Thiel, A. Wander and P. Sherwood, *J. Phys. Chem. A*, 2009, **113**, 11856–11865.
28 F. Weigend and R. Ahlrichs, *Phys. Chem. Chem. Phys.*, 2005, **7**, 3297.
29 H. Nakanishi, H. Morita and S. Nagakura, *Bull. Chem. Soc. Jpn.*, 1978, **51**, 1723–1729.
30 T. Skalický, C. Chollet, N. Pasquier and M. Allan, *Phys. Chem. Chem. Phys.*, 2002, **4**, 3583–3590.
31 R. Dressler and M. Allan, *J. Chem. Phys.*, 1987, **87**, 4510.
32 R. Janečková, D. Kubala, O. May, J. Fedor and M. Allan, *Phys. Rev. Lett.*, 2013, **111**, 213201.
33 G. Gallup, P. Burrow and I. Fabrikant, *Phys. Rev. A*, 2009, **79**, 042701.
34 J. R. B. Gomes and M. A. V. R. da Silva, *J. Phys. Chem. A*, 2006, **110**, 13948–13955.
35 J. E. Bassett and E. Whittle, *Int. J. Chem. Kinet.*, 1976, **8**, 859–876.
36 G. C. Pimentel, F. M. G Tablas, J. Hartmann and E. Whittle, *Int. J. Chem. Kinet.*, 1976, **8**, 877–882.
37 K. J. Muyskens, J. R. Alsum, T. A. Thielke, J. L. Boer, T. R. Heetderks and M. A. Muyskens, *J. Phys. Chem. A*, 2012, **116**, 12305–12313.
38 B. Ómarsson, E. H. Bjarnason, S. A. Haughey, T. A. Field, A. Abramov, P. Klüpfel, H. Jónsson and O. Ingólfsson, *Phys. Chem. Chem. Phys.*, 2013, **15**, 4754–4766.
39 M. Heni and E. Illenberger, *J. Chem. Phys.*, 1985, **83**, 6056.
40 T. Oster, *PhD thesis*, Freie Universität Berlin, 1987.
41 E. Illenberger and M. Meinke, *J. Phys. Chem. A*, 2014. DOI: 10.1021/jp503129z.
42 I. Martin, M. Bertin, A. Domaracka, R. Azria, E. Illenberger and A. Lafosse, *Int. J. Mass. Spectrom.*, 2008, **277**, 262–268.
43 M.-C. Yoon, Y. S. Choi and S. K. Kim, *Chem. Phys. Lett.*, 1999, **300**, 207–212.
44 H. P. Upadhyaya, A. Kumar and P. D. Naik, *J. Chem. Phys.*, 2003, **118**, 2590.
45 I. Bald, J. Langer, P. Tegeder and O. Ingólfsson, *Int. J. Mass. Spectrom.*, 2008, **277**, 4–25.
46 O. Ingólfsson, F. Weik and E. Illenberger, *Int. Rev. Phys. Chem.*, 1996, **15**, 133–151.
47 M. R. Nimlos, J. A. Soderquist and G. B. Ellison, *J. Am. Chem. Soc.*, 1989, **111**, 7675–7681.
48 H. Abdoul-Carime, M. A. Huels, E. Illenberger and L. Sanche, *J. Am. Chem. Soc.*, 2001, **123**, 5354–5355.

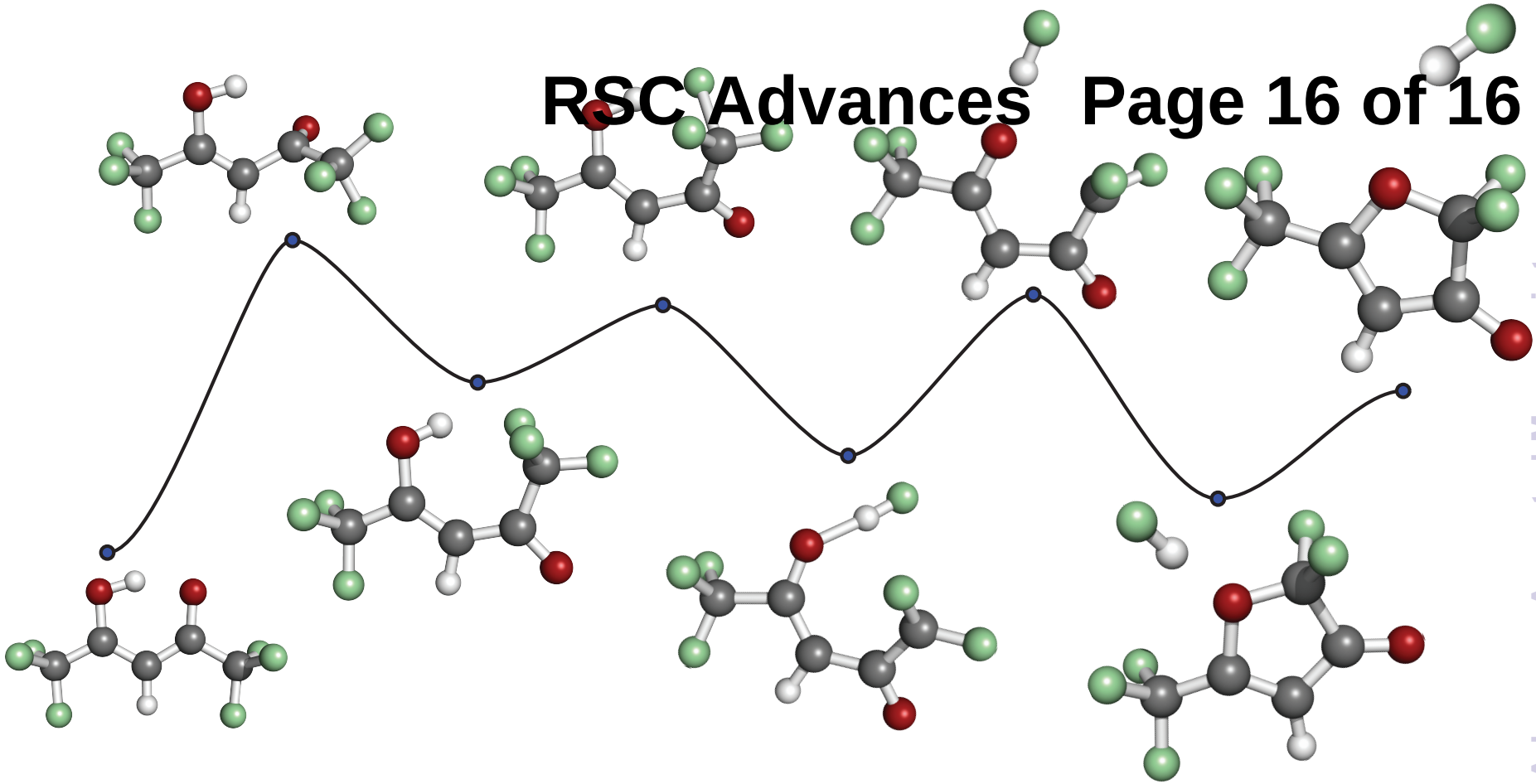

# Influence of fluorination on the negative ion resonances and dissociation dynamics in electron attachment to acetylacetone, trifluoroacetylacetone and hexafluoroacetylacetone are explored through calculations and experiments